IOSR Journal of Mechanical and Civil Engineering (IOSR-JMCE)
e-ISSN: 2278-1684, p-ISSN: 2320-334X, Volume 23, Issue 5 Ser. I (Sep. – Oct. 2026), PP 70-84
www.iosrjournals.org

Spatial Distribution of Wheat Threshed Mixture and Theoretical Cleaning-Airflow Velocity Boundaries in a Single Longitudinal Axial-Flow Combine Harvester

Peng Liu[1], Xiangyou Wang[2] , Chengqian Jin[2,3,*], Mingming Liu [4], Zongjing Huang[1], Aihai Li[1]
[1] *School of Mechanical and Electrical Engineering, Weifang University of Science and Technology, Weifang 262700, China*
[2] *School of Agricultural Engineering and Food Science, Shandong University of Technology, Zibo 255000, China*
[3] *Nanjing Institute of Agricultural Mechanization, Ministry of Agriculture and Rural Affairs, Nanjing 210014, China*
[4] *Mechanical and Electronic Engineering College, Shandong Agriculture and Engineering University, Jinan 250100, China*

Abstract: *During the operation of a single longitudinal axial-flow wheat combine harvester, the threshed mixture is often unevenly distributed on the cleaning sieve, leading to locally thick material layers, increased cleaning losses, and higher impurity content. To address this problem, this study investigated the spatial distribution characteristics of wheat threshed mixture on the cleaning sieve and measured the critical terminal velocities of key components. Based on these results, theoretical cleaning-airflow velocity boundaries were analyzed. A self-developed 4LZ-2.5 test bench was used. The cleaning sieve was divided into six regions using a full-width grid sampling method. The regional distribution characteristics of plump grains, unthreshed heads, long stalks, short stalks, and chaff and light impurities were quantitatively characterized. Meanwhile, a critical terminal velocity test apparatus was used to determine the critical terminal velocities of the main components. The results showed that, under the single longitudinal axial-flow condition, the wheat threshed mixture exhibited a distinct front-concentrated and rear-sparse longitudinal distribution pattern and a right-biased transverse deposition pattern on the cleaning sieve. In particular, plump grains accounted for 70.52% of the material in the front-right region of the sieve, namely Zone 1-a, suggesting that this region may be prone to locally high material accumulation and increased airflow penetration resistance. The average critical terminal velocities of plump grains, long stalks, unthreshed heads, short stalks, and chaff and light impurities were 7.51, 6.13, 5.65, 4.22, and 2.12 m/s, respectively. The critical terminal velocity of unthreshed heads was lower than those of plump grains and long stalks, indicating that unthreshed heads could be regarded as the sensitive recoverable component for defining the upper boundary of cleaning airflow velocity. Considering both the removal requirement of chaff and light impurities and the recovery requirement of unthreshed heads, the mean-based theoretical control range of cleaning airflow velocity was preliminarily estimated as 2.12-5.65 m/s. The analysis further indicated that conventional uniform airflow is difficult to simultaneously satisfy the airflow penetration requirement in high-load regions and the low-loss cleaning requirement in low-load regions. Therefore, a zone-differentiated airflow distribution strategy may improve the matching relationship between cleaning airflow and the non-uniform material distribution on the sieve. These results provide data support and a theoretical reference for parameter setting and structural optimization of non-uniform airflow cleaning systems in single longitudinal axial-flow wheat combine harvesters.*
Keywords*: longitudinal axial-flow combine, threshed mixture, sieve-load distribution, critical terminal velocity, cleaning airflow velocity boundary*

Date of Submission: 13-09-2026 Date of Acceptance: 25-09-2026

INTRODUCTION

Wheat is one of the most important cereal crops worldwide and plays a crucial role in ensuring food security and a stable grain supply. Shiferaw et al. pointed out that wheat provides approximately 20% of global dietary calories and protein, and that its production stability is closely related to global food security [1]. With the continuous development of agricultural mechanization, combine harvesters have become the main equipment for wheat harvesting. Their harvesting performance directly affects grain loss, impurity content, and the quality of subsequent storage and processing. The cleaning system of a combine harvester is generally composed of a fan, cleaning sieves, and related airflow-guiding components. It separates grains from glumes, stalks, unthreshed heads, and other impurities through the coupled effects of airflow separation and sieve vibration. Liang and Wada reviewed the development of combine harvester cleaning systems and indicated that the cleaning device is one of the key components affecting operating quality, adaptability, and automation level [2]. Recent measurements of airflow velocity profiles over the upper and lower sieves of wheat combine harvesters further confirmed that fan speed, wind-board position, and sieve opening influence the spatial distribution of cleaning airflow, and that airflow-profile evaluation is necessary for reducing grain losses and impurity content [3].

In a single longitudinal axial-flow combine harvester, the crop is threshed and separated between the longitudinally arranged threshing drum and the concave sieve after being fed into the machine. Compared with conventional tangential-flow or transverse-flow structures, the longitudinal axial-flow threshing and separating unit is characterized by a longer threshing path, stronger separation capacity, and better adaptability; therefore, it has been widely used in wheat combine harvesters. Yuan et al. designed and tested a tangential–longitudinal axial-flow threshing and separating unit for wheat, showing that the longitudinal axial-flow structure can meet the requirements of low-loss and high-efficiency wheat harvesting [4]. However, during the operation of a longitudinal axial-flow drum, the crop undergoes helical conveying along the drum axis and is simultaneously affected by the drum teeth, guide vanes, and centrifugal force. Consequently, when the threshed mixture passes through the concave sieve and falls onto the cleaning sieve, a non-uniform spatial distribution may occur. Milišauskas et al. studied crop flow control in a longitudinal axial-flow threshing unit and reported that guide vanes significantly affect crop movement paths and separation processes inside the axial-flow drum. Improper crop flow control may increase grain loss and reduce harvesting quality [5]. Therefore, for single longitudinal axial-flow wheat combine harvesters, the spatial distribution of the threshed mixture on the cleaning sieve is an important prerequisite affecting the subsequent airflow cleaning process.

The cleaning process is essentially a gas–solid separation process. A suitable airflow velocity should remove light impurities while preventing grains or recoverable unthreshed heads from being blown out of the cleaning chamber. Critical terminal velocity is an important aerodynamic parameter for determining cleaning airflow parameters. Gorial and O'Callaghan measured the aerodynamic properties of various grain and straw materials and pointed out that particle size, shape, and density significantly affect critical terminal velocity and airflow separation behavior [6]. Khoshtaghaza and Mehdizadeh measured the critical terminal velocity and drag coefficient of wheat kernels and straw materials, suggesting that the difference in critical terminal velocity between wheat kernels and straw can provide an important basis for setting airflow separation parameters [7]. Zewdu also reported that moisture content and material morphology affect the critical terminal velocity of tef grain and straw [8]. These studies provide an important foundation for setting cleaning airflow parameters. However, most critical terminal velocity measurements have been conducted under relatively ideal vertical airflow conditions using individual particles or small amounts of material. Relatively few studies have considered local material accumulation and non-uniform load conditions on an actual cleaning sieve. Recent numerical and experimental studies have also treated air-and-screen cleaning as a coupled gas-solid process, in which airflow velocity, particle motion, local mixture accumulation, and material-layer resistance jointly determine impurity removal and grain loss [9, 10].

In addition to the aerodynamic properties of the materials themselves, the airflow field in the cleaning chamber and its interaction with the material layer also significantly affect cleaning performance. Streicher et al. measured airflow velocities at multiple positions in the cleaning chamber during wheat combine harvesting and found that, as material flow increased, the average airflow velocity in some regions of the cleaning sieve decreased. This result indicates that material load can inversely affect airflow distribution and penetration capacity [11]. Craessaerts et al. established a prediction model for material-other-than-grain content during the combine cleaning process and pointed out that the cleaning process is nonlinear and uncertain, being affected by operating parameters, material flow, and machine state [12]. Badretdinov et al. developed a mathematical model of the working process of a fan–sieve cleaning system in grain combine harvesters, further demonstrating the coupling relationship among sieve motion, airflow velocity, and material movement [13]. In recent years, studies on multi-duct cleaning devices and fan structure optimization have also shown that improving the uniformity of cleaning airflow distribution can help reduce sieve losses and impurity content [14, 15]. Nevertheless, these studies have mainly focused on cleaning system structure, airflow field distribution, or control models, whereas insufficient attention has been paid to the local high-load distribution of wheat threshed mixture formed on the cleaning sieve in single longitudinal axial-flow harvesters and its matching relationship with the critical terminal velocities of key components. Recent CFD-based and airflow-field investigations further show that uneven airflow over the sieve shoe is a common cause of unstable separation quality, and that the airflow velocity may vary considerably along both the longitudinal and transverse directions of the sieve [9]. The installation of auxiliary airflow structures, such as cross-flow fans and front-blowing/rear-suction devices, has been shown to improve multi-dimensional airflow distribution and reduce airflow non-uniformity in combine cleaning chambers [16, 17].

Previous studies have tended to examine the spatial distribution of threshed mixture and material critical terminal velocity separately. One group of studies has focused on measuring the terminal velocities of grains, stalks, glumes, and other impurities to determine the airflow velocity range for cleaning, whereas another group has focused on the effects of fans, air ducts, sieve motion, or control methods on cleaning performance. However, in single longitudinal axial-flow wheat combine harvesters, the threshed mixture does not fall uniformly onto the cleaning sieve. Instead, it is affected by helical conveying, tangential throwing, and centrifugal separation of the drum, which may lead to local high-load regions at the front or on one side of the sieve. If uniform sieve load is assumed when setting cleaning airflow parameters, this may result in insufficient airflow penetration in high-load regions and excessive airflow in low-load regions, thereby affecting the balance between impurity removal and low-loss cleaning. Therefore, it is necessary to combine the spatial distribution characteristics of the wheat threshed mixture on the cleaning sieve with the critical terminal velocities of key components to establish a basis for cleaning airflow parameters under non-uniform load conditions. Moreover, airflow-field control based on load distribution has recently been proposed to connect regional material load, airflow regulation, and cleaning performance, which supports the necessity of combining sieve-load distribution with cleaning-airflow boundary analysis [18].

The novelty of this study lies in coupling the regional deposition characteristics of wheat threshed components on the cleaning sieve with their suspension characteristics to determine theoretical airflow velocity boundaries under non-uniform deposition conditions. To address these issues, this study focuses on the cleaning system of a single longitudinal axial-flow wheat combine harvester. A self-developed 4LZ-2.5 longitudinal axial-flow threshing and cleaning test bench was used to conduct experiments on the spatial distribution of wheat threshed mixture on the cleaning sieve and the critical terminal velocities of major components. The specific objectives were: (1) to quantitatively characterize the regional distribution of wheat threshed mixture in different regions of the cleaning sieve using a full-width grid sampling method and to clarify the longitudinal distribution and transverse offset loading pattern under the single longitudinal axial-flow condition; (2) to determine the critical terminal velocities of plump grains, unthreshed heads, long stalks, short stalks, and chaff and light impurities, and to identify the sensitive component limiting the upper boundary of cleaning airflow velocity; and (3) to analyze the theoretical control boundaries of cleaning airflow velocity and discuss a conceptual zone-differentiated airflow distribution strategy by combining local sieve load distribution with component critical terminal velocity. This study provides a data basis and theoretical reference for parameter setting and structural optimization of non-uniform airflow cleaning systems in single longitudinal axial-flow wheat combine harvesters.

MATERIALS AND METHODS

2.1 Test Bench and Measurement Devices

2.1.1 4LZ-2.5 Threshing and Cleaning Test System

The experiment was conducted on a self-developed 4LZ-2.5 longitudinal axial-flow threshing and cleaning test bench, as shown in Figure 1. The test bench mainly consisted of a material conveying device, a feeding device, a single longitudinal axial-flow threshing and separating unit, an air-and-screen cleaning device, and a data acquisition and control system. It was designed to simulate the threshing, separation, and cleaning processes of a wheat combine harvester under stable feeding conditions.

The test bench featured a modular structural design, allowing each working unit to be independently adjusted and controlled. The system was equipped with a PLC-based human-machine interface platform, which enabled stepless adjustment of key parameters, including threshing drum rotational speed, centrifugal fan speed, and cleaning sieve drive shaft speed—via variable frequency drives, along with real-time monitoring of these parameters. The adjustable range of the threshing drum rotational speed was 0-1100 *r/min*. This design reduced the influence of mechanical coupling of multiple components and external environmental variations on the test results, thereby providing relatively stable experimental conditions for analyzing the spatial distribution of threshed mixture on the sieve and determining cleaning airflow parameters under single longitudinal axial-flow conditions.

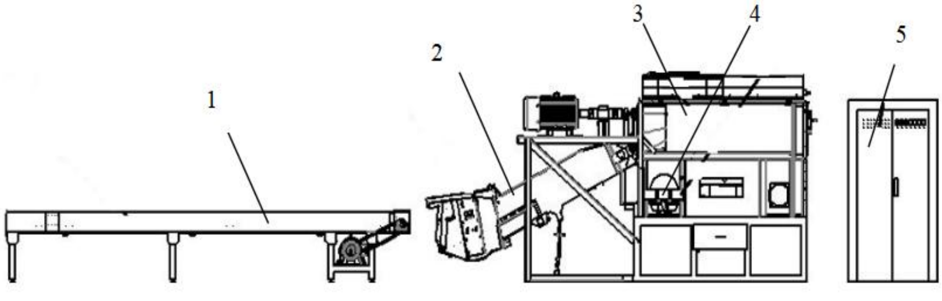

1. Material conveying device 2. Feeding device 3. Single longitudinal axial-flow threshing and separating unit 4. Air-screen cleaning device 5. Data acquisition and control system.

Figure 1. 4LZ-2.5 longitudinal axial-flow threshing and cleaning test bench.

The core threshing and separating component of the test bench adopted a combined configuration consisting of a spike-tooth longitudinal axial-flow drum and a grid concave, as shown in Figure 2. During operation, wheat plants were fed into the threshing and separating unit through the feeding device. Under the action of the high-speed rotating drum, the plants were subjected to complex mechanical interactions, including impact, rubbing, and combing, thereby separating grains from heads and stalks. The threshed mixture passed through the openings of the concave and entered the cleaning device. Its spatial distribution was simultaneously governed by axial conveying and radial throwing of the drum.

Along the axial direction of the drum, the crop successively passed through the feeding section, threshing section, and separating section under the action of the helical guide vanes, corresponding to Sections 1, 2, and 3 in Figure 2(a). As the material moved backward along the axial direction, different components were gradually separated and dropped through the concave in different functional sections, thereby affecting the distribution of the threshed mixture in the longitudinal direction of the cleaning sieve. Along the radial direction of the drum, the tangential velocity and centrifugal effect generated by the clockwise rotation of the drum caused the threshed mixture to exhibit a pronounced lateral throwing tendency. According to the rotation direction of the drum shown in Figure 2(b), the descending side of the drum was defined as side a, whereas the ascending side was defined as side b. Because the threshed mixture was affected by radial throwing during falling, the deposited quantities on sides a and b may differ, resulting in a transverse offset loading pattern on the cleaning sieve.

The combined effects of axial conveying and radial throwing constitute the primary mechanism underlying the non-uniform spatial distribution of the threshed mixture beneath the single longitudinal axial-flow threshing and separating unit. They also provide the structural and physical basis for dividing the cleaning sieve into different sampling regions in subsequent experiments.

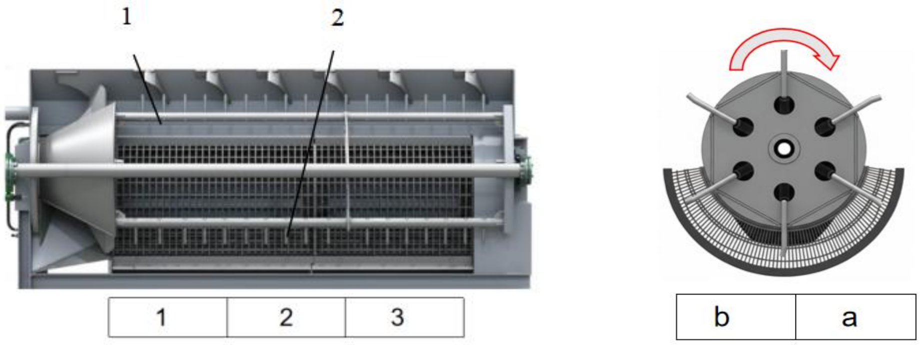

1-drum rasp bars, 2-Concave.

(a) Axial view of the threshing drum; (b) Radial view of the threshing drum;

Figure 2. Single longitudinal axial-flow threshing and separating unit.

The air-and-screen cleaning device is the core component for separating grains from impurities in the wheat threshed mixture. Its working process mainly relies on the coupled effects of the reciprocating vibration of the cleaning sieve and the airflow field generated by the centrifugal fan [19-21]. As shown in Figure 3, after the multiphase mixture discharged from the threshing and separating unit falls onto the cleaning sieve, it is conveyed backward along the longitudinal direction of the sieve by sieve vibration, while being subjected to an obliquely upward airflow generated by the centrifugal fan and guided through the air duct. Owing to differences in aerodynamic characteristics, including density, shape, size, and critical terminal velocity, different components are gradually separated through the coupled effects of sieve motion and airflow.

During the cleaning process, dense plump grains and some short-broken materials pass through the sieve openings and enter the grain-collecting screw conveyor. Unthreshed heads slide from the tail sieve into the rethreshing screw conveyor for secondary threshing, whereas components with low critical terminal velocities, such as chaff, broken leaves, and light impurities, are blown out of the cleaning chamber by the airflow [22-24]. Airflow deflector strips are installed inside the cleaning device, and their deflection angle can be adjusted to change the local airflow direction and velocity distribution, thereby regulating, to some extent, the airflow intensity in different regions of the sieve. This structure provides an experimental basis for investigating the matching relationship between cleaning airflow and the spatial distribution of the threshed mixture, as well as for discussing zone-differentiated airflow control strategies under non-uniform load conditions.

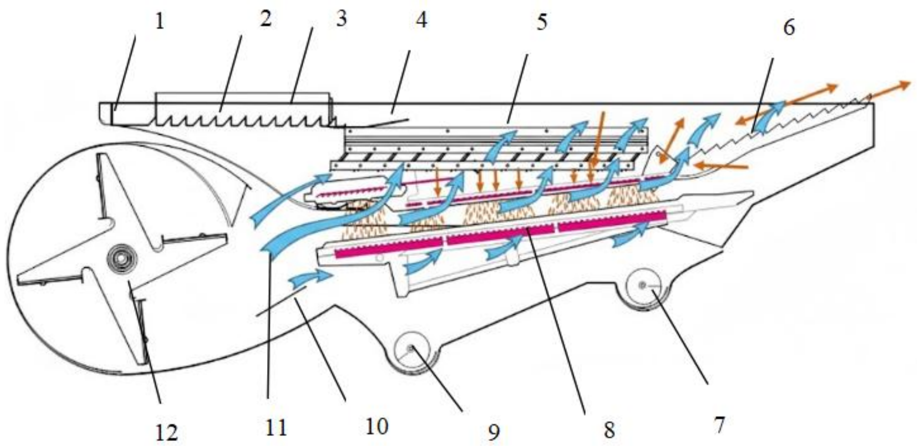

1-Sorting sieve; 2-Vibration plate; 3-Deflector strip; 4- Finger sieve; 5-Chaffer sieve; 6-Tail sieve; 7-Rethreshing screw conveyor; 8-Mesh sieve; 9-Grain-collecting screw conveyor; 10-Air duct; 11-Airflow direction; 12-Fan.

Figure 3. Air-and-screen cleaning device.

2.1.2 Critical Terminal Velocity Test Apparatus

To quantify the aerodynamic characteristics of the main components of the wheat threshed mixture, a critical terminal velocity test apparatus was used to determine the critical terminal velocities of the main components, as shown in Figure 4. The apparatus mainly consisted of a variable-frequency fan, a flow-stabilizing section, a transparent conical observation tube, a ruler, and an orifice flowmeter. During testing, the variable-frequency fan supplied a continuously adjustable vertical upward airflow. The flow-stabilizing section was used to reduce airflow turbulence inside the observation tube, the transparent conical observation tube facilitated visual observation of the suspended state of the material, and the orifice flowmeter was used to measure the dynamic pressure of the test airflow.

The basic principle of the critical terminal velocity test is the force equilibrium of material particles in a vertical upward airflow. When the gravitational force acting on the material is balanced by the aerodynamic drag force, the material remains in a relatively stable suspended state inside the observation tube. The corresponding airflow velocity is defined as the critical terminal velocity of the material. In this study, critical terminal velocity refers to the critical airflow velocity at which the material reaches a relatively stable suspended state in a vertical upward airflow, denoted as V_p. Plump grains, unthreshed heads, long stalks, short stalks, and chaff and light impurities were selected as typical components and tested independently. Before testing, samples of each component were manually screened to remove damaged, moldy, or morphologically abnormal samples, thereby reducing the influence of sample heterogeneity on the measurement results.

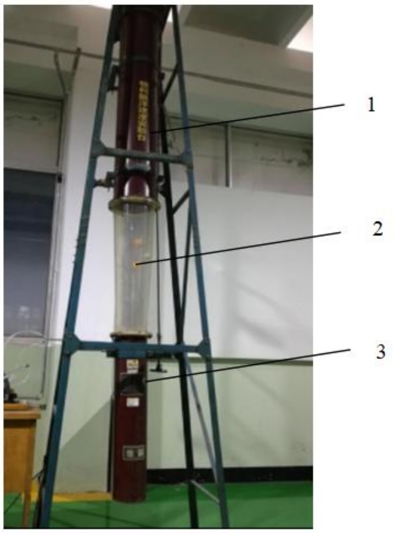

1-Flow-field component;2-Test component; 3-Airflow velocity adjustment component.

Figure 4. Critical terminal velocity test apparatus.

2.2 Test Materials

The wheat variety 'Linmai No. 4', grown at the wheat experimental base in Hedong District, Linyi City, Shandong Province, China, was used as the test material. The experimental materials were collected from mature wheat plants. To ensure consistency in sample condition and repeatability of the test results, wheat plants with uniform growth and no obvious diseases or insect damage were manually harvested. The complete stalks and ears were retained intact to simulate the feeding state during field combine harvesting.

Before the experiment, the main agronomic and physical parameters of the test wheat were measured using the five-point sampling method according to GB/T 5262-2008 General Rules for the Determination of Test Conditions for Agricultural Machinery. The results are listed in Table 1. The plant mass per unit area was 1.60 kg/m^2, which was used in the subsequent calculation of the simulated feeding speed of the test bench. Given that moisture content significantly influences material density, critical terminal velocity, and airflow separation characteristics, the moisture contents of different components were determined using the oven-drying method before the test. The average moisture contents of stalks, unthreshed heads, and plump grains were 14.00%, 12.00%, and 13.21%, respectively. The average moisture content of light impurities, including chaff and broken leaves, was approximately 18.50%, These parameters were used to define the physical state of the materials for critical terminal velocity measurement and served as the basis for subsequent analysis of cleaning airflow parameters.

Table 1. Main agronomic and physical parameters of the test wheat.

Parameter Name	**Parameter Value**
Wheat Variety	'Linmai No. 4'
Growth period/ d	235
Plant Mass per Unit Area/ (kg/m^2)	1.60
Grain yield per unit area / (kg/m^2)	0.647
Ear length/ mm	77.6±15.0
Natural plant height/ *mm*	649±15
Straw-to-grain ratio	0.78
Grain moisture content/ %	13.21
Thousand-grain weight/ g	37.6

2.3 Test Methods

2.3.1 Sampling Method for Sieve Material Distribution

To quantitatively characterize the spatial distribution of wheat threshed mixture on the cleaning sieve under the single longitudinal axial-flow condition, a full-width grid sampling method was used for regional collection of the falling threshed mixture [20, 25-29]. This method allows simultaneous acquisition of distribution information in both the longitudinal and transverse directions of the cleaning sieve, and was used to analyze the longitudinal attenuation pattern and transverse offset loading characteristics of the threshed mixture on the cleaning sieve.

According to the structural functional sections of the single longitudinal axial-flow threshing drum and the material movement direction, a two-dimensional sampling coordinate system was established on the cleaning sieve. Along the axial direction of the drum, namely the longitudinal direction of the sieve, the sieve surface was divided into three regions, denoted as Regions 1, 2, and 3, corresponding to the feeding section, threshing section, and separating section of the threshing drum, respectively. These regions were used to analyze the distribution variation of the threshed mixture along the material movement direction. Along the transverse direction of the sieve, based on the tangential throwing and centrifugal separation caused by the clockwise rotation of the drum, the sieve surface was divided into two lateral regions, denoted as a and b. The descending side of the drum, namely the right side, was defined as Region a, whereas the ascending side, namely the left side, was defined as Region b. This definition was consistent with the lateral division shown in the radial view of the drum in Figure 2.

Based on the above regional divisionsix equal-area collecting boxes were arranged beneath the corresponding regions of the cleaning sieve, corresponding to Zone 1-a, Zone 1-b, Zone 2-a, Zone 2-b, Zone 3-a, and Zone 3-b, as shown in Figure 5. During the experiment, after the test bench reached stable feeding and operating conditions, the threshed mixture falling from each region was collected synchronously. Sampling was performed after the test material of the preset length on the conveyor belt had completely passed through the threshing and separating unit. Prior to each test replicate, the collecting boxes, sieve surface, and related residues were cleaned to reduce the influence of residual material from previous tests.

After collection, the samples from each region were manually separated into plump grains, unthreshed heads, long stalks, short stalks, and chaff and light impurities, and the mass of each component was measured separately. The mass percentage of each component in the corresponding region was calculated according to Eq. (1):

$$P_{ij,k}=\frac{m_{ij,k}}{\sum_{r=1}^{n} m_{ij,r}}\times 100\% \quad (1)$$

where $P_{ij,k}$ is the mass percentage of the *k*-th component in the *i*-th longitudinal region and the *j*-th transverse side region, %; $m_{ij,k}$ is the mass of the *k*-th component in the *i*-th longitudinal region and the *j*-th transverse side region, *g*. $m_{ij,r}$ is the mass of the r-th component in this region, *g*; *i*=1,2,3 represents the regions corresponding to the feeding section, threshing section, and separating section, respectively; *j*=a,b represents the descending side and ascending side of the drum, respectively; and n is the number of separated components.

To reduce random errors, each test was repeated three times, and the average value was used. The obtained data were used for subsequent analysis of the longitudinal distribution, transverse offset loading, and spatial distribution differences among different components of the wheat threshed mixture on the cleaning sieve.

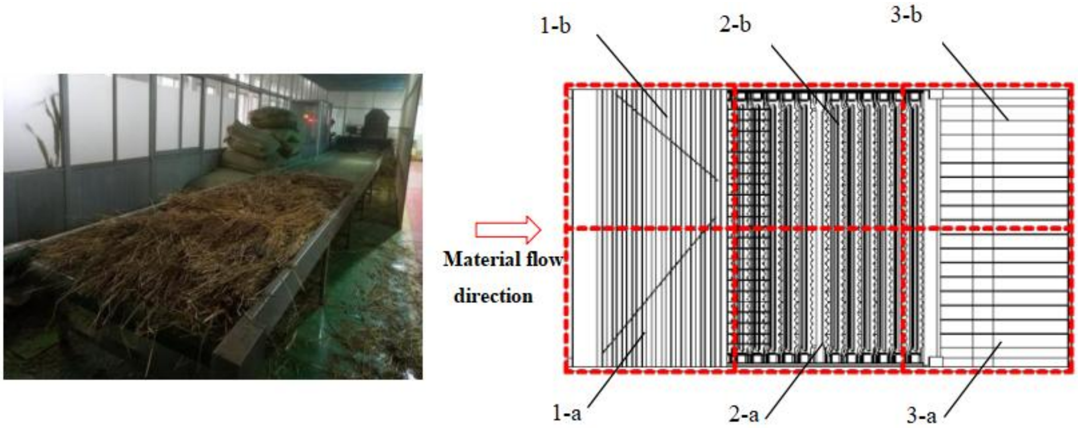

（a） (b)

Figure 5. Grid division of sampling regions for threshed mixture on the cleaning sieve: (a) field view of the threshing test bench; (b) schematic diagram of sieve grid division.

2.3.2 Test Parameter Setting and Basis

To obtain the sieve distribution characteristics of the threshed mixture from a single longitudinal axial-flow wheat combine harvester under rated operating conditions, the test conditions were set according to the design parameters of the 4LZ-2.5 combine harvester. The feed velocity of the test bench was determined from the target feed rate, simulated cutting width, and plant mass per unit area, so that the feeding state of the bench test was consistent with the rated field operating conditions. The instantaneous feed rate was expressed as:

$$q = B \cdot \rho_{area} \cdot v \quad (2)$$

where *q* is the feed rate of the test bench, *kg/s*; *B* is the simulated cutting width, *m*; ρ_{area} is the plant mass per unit area of wheat, *kg/m²*; and v is the simulated operating velocity, namely the conveyor belt velocity, *m/s*. In this study, the rated feed rate of the 4LZ-2.5 combine harvester was 2.5 *kg/s*, the simulated cutting width was 1.8 *m*, and the plant mass per unit area of wheat was 1.60 *kg/m²*. The simulated operating velocity was computed using Eq. (2):

$$v = \frac{q}{B\cdot\rho_{\mathrm{area}}} = \frac{2.5}{1.8\times 1.60} \approx 0.87\ m/s \quad (3)$$

Thus, the conveyor belt velocity was set to 0.87 *m/s*, and the effective spreading length of the material on the conveyor belt was set to 3 *m* to ensure that the test bench operated under stable load conditions. Considering the trade-off between threshing completeness and grain damage during wheat threshing, and referring to the drum rotational speed ranges reported in studies on axial-flow or longitudinal axial-flow wheat threshing and separating units, the threshing drum rotational speed was set to 950 *r/min* according to the design condition of the 4LZ-2.5 test bench.

During the sieve distribution sampling test, the air-and-screen cleaning device was operated under a fixed baseline condition. The crank rotational speed of the vibrating sieve, fan rotational speed, air-gate opening, and chaffer sieve opening were kept constant in all test replicates and were not used as experimental variables. According to the adjustable ranges of the cleaning operation parameters of the test bench, the above parameters could be adjusted within 50-600 *r/min*, 500-2600 *r/min*, 0-18°, and 0-36 *mm*, respectively. Since this study focused on the spatial distribution characteristics of the threshed mixture caused by the single longitudinal axial-flow threshing and separating unit, as well as the matching relationship between this distribution and the terminal velocities of key components, the cleaning device parameters were controlled as fixed baseline conditions and excluded as variables for factorial analysis. The main operating parameters are listed in Table 2.

Table 2. Key operating parameters of the threshing and cleaning test bench.

Parameter Name	Symbol	Parameter Value
Rated feed rate / (*kg/s*)	*q*	2.5
Threshing drum rotational speed / (*r/min*)	*n*	950
Simulated operating velocity / (*m/s*)	*v*	0.87
Effective spreading length / *m*	*L*	3
Simulated cutting width / *m*	*B*	1.8

2.3.3 Data Processing and Critical Terminal Velocity Calculation

To quantitatively characterize the aerodynamic properties of the different components of the wheat threshed mixture, the critical terminal velocities of each component were measured using the critical terminal velocity test apparatus. During the test, when each sample reached a relatively stable suspended state in the vertical upward airflow, the corresponding dynamic pressure was recorded, and the critical terminal velocity was calculated according to the pressure-velocity conversion relationship.

To reduce random errors, the dynamic pressure of each sample was measured three times, and the average value was used for calculation:

$$P_d = \frac{P_{d1}+P_{d2}+P_{d3}}{3} \quad (4)$$

where P_d is the mean dynamic pressure (*mm* H_2O), and P_{d1}, P_{d2}, and P_{d3} are the dynamic pressure values obtained from three repeated measurements (*mm* H_2O).

According to the Pitot tube principle, the relationship between airflow velocity and dynamic pressure is expressed as:

$$V_p = \sqrt{\frac{2P}{\rho}} \quad (5)$$

where V_p is the critical terminal velocity (*m/s*), P is the dynamic pressure (*Pa*), and ρ is the air density (*kg/m*^{3}). The test was conducted under standard laboratory conditions, with an air density of ρ=1.205 *kg/m*^{3}. Since the dynamic pressure reading P_d was recorded in mm H_2O and 1 *mm* H_2O≈9.80665 *Pa*, the following conversion was used:

$$P = 9.80665 P_d \quad (6)$$

Substituting Eq. (6) into Eq. (5) gives:

$$V_p = \sqrt{\frac{2\times 9.80665 P_d}{1.205}} \approx 4.03\sqrt{P_d} \quad (7)$$

For practical engineering calculations, the coefficient 4.03 in Eq. (7) was approximated as 4 for practical engineering calculations. Therefore, the critical terminal velocity calculation equation was simplified as:

$$V_p = 4\sqrt{P_d} \quad (8)$$

Where P_d is expressed in *mm* H_2O and V_p is expressed in *m/s*.

2.3.4 Statistical Analysis

Initial data organization and processing were performed using Microsoft Excel. For the sieve spatial distribution tests, each group was repeated three times, and the results were expressed as mean values to describe the variation trends in the mass percentages of different components in different sieve regions. For the critical terminal velocity tests, 50 samples were randomly selected for each component, and the results were expressed as mean±standard deviation (SD), range, and coefficient of variation (CV). One-way analysis of variance (ANOVA) was performed using SPSS 26.0 to assess differences in critical terminal velocity among different components, and Duncan's multiple range test was used for post hoc comparisons. All statistical analyses were performed at a significance level of $P < 0.05$.

RESULTS AND DISCUSSION

3.1 Spatial Distribution Patterns of Wheat Threshed Mixture

3.1.1 Composition Characteristics and Macroscopic Offset Analysis

Under the rated operating conditions of the 4LZ-2.5 longitudinal axial-flow threshing and cleaning test bench, with a feed rate of 2.5 *kg/s* and a threshing drum rotational speed of 950 r/min, wheat plants were separated into a multi-component threshed mixture after threshing and separation. According to material morphology and separation characteristics during the cleaning process, the threshed mixture was classified into five components: plump grains, unthreshed heads, long stalks, short stalks, and chaff and light impurities.

To quantitatively analyze the spatial distribution characteristics of each component on the cleaning sieve, the full-width grid sampling method described in Section 2.3.1 was adopted. The cleaning sieve was divided into six characteristic zones, namely Zone 1-a, Zone 1-b, Zone 2-a, Zone 2-b, Zone 3-a, and Zone 3-b. The samples collected from each zone were manually separated and weighed. The mass percentages of different components in each zone are shown in Table 3, and the spatial distribution trend is illustrated in Figure 6.

As shown in Table 3, the distribution of the wheat threshed mixture on the cleaning sieve was clearly non-uniform under the single longitudinal axial-flow condition. In the front-right region of the sieve, namely Zone 1-a, the mass percentage of plump grains reached 70.52%, which was markedly higher than that in the other zones, indicating that this zone was the main region of grain deposition. In contrast, the mass percentage of plump grains in the front-left region, Zone 1-b, was 34.25%, which was much lower than that in Zone 1-a. This result indicates a pronounced transverse offset loading pattern at the front of the cleaning sieve.

In the longitudinal direction, the mass percentage of plump grains generally decreased along the material movement direction on the cleaning sieve. On side a, it decreased from 70.52% in Zone 1-a to 29.25% in Zone 3-a. On side b, it decreased from 34.25% in Zone 1-b to 25.40% in Zone 3-b. This result indicates that plump grains were mainly concentrated in the front region of the cleaning sieve. As the material moved backward along the sieve surface, the proportion of plump grains gradually decreased, whereas the proportions of stalks and chaff and light impurities increased relatively.

In the transverse direction, differences in component composition were observed between sides a and b. Zone 1-a showed a relatively high mass percentage of plump grains, whereas the mass percentage of chaff and light impurities in Zone 1-b reached 47.24%, much higher than the 24.30% observed in Zone 1-a at the same longitudinal position. This indicates that components with different physical properties exhibited lateral separation and offset as they passed through the concave and were deposited on the cleaning sieve.

Overall, during the single longitudinal axial-flow threshing and separation process, the wheat threshed mixture formed a spatial distribution characterized by a front-concentrated and rear-sparse deposition pattern and a right-biased transverse deposition pattern, with relatively more chaff and light impurities distributed on the left side. These results indicate that both the material load and component composition varied among different sieve regions. If uniform airflow is used for cleaning, it may be difficult to simultaneously satisfy the airflow penetration requirement in high-load regions and the low-loss cleaning requirement in low-load regions.

Table 3. Mass percentage of wheat threshed components in different sieve zones.

Zone	Plump Grains /(%)	Unthreshed Heads / (%)	Long Stalks / (%)	Short Stalks / (%)	Chaff and light impurities / (%)
1-a	70.52	3.19	1.20	0.80	24.30
1-b	34.25	9.84	4.72	3.94	47.24
2-a	37.80	2.36	11.81	8.27	39.76
2-b	38.74	2.37	10.67	6.32	41.90
3-a	29.25	1.19	13.04	11.07	45.45
3-b	25.40	1.59	16.27	17.06	39.68

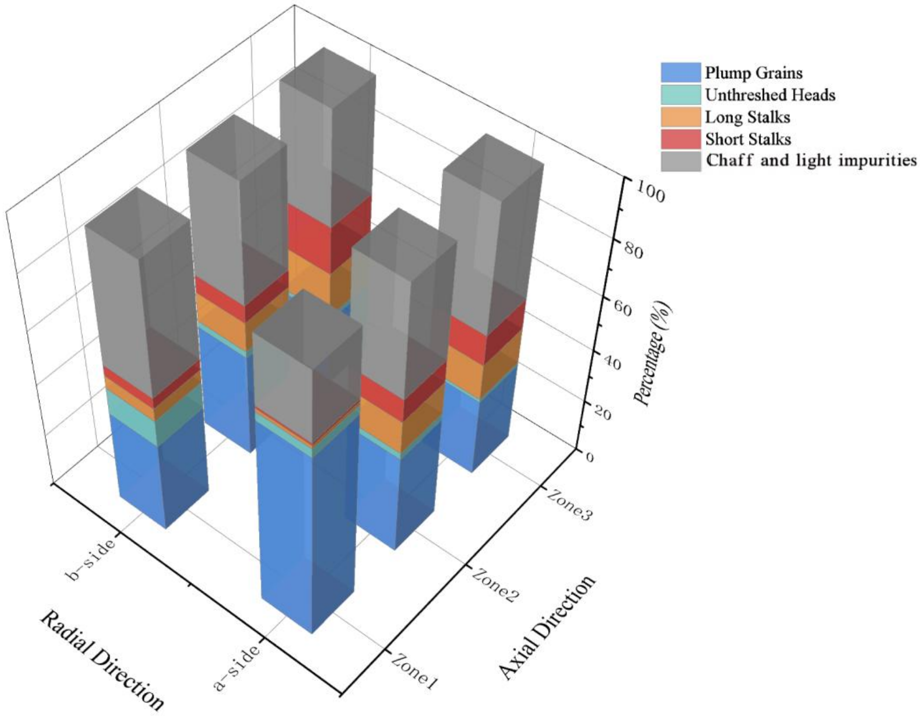

Figure 6. Three-dimensional spatial distribution of mass percentages of wheat threshed components.

3.1.2 Mechanism of Component Spatial Distribution on the Cleaning Sieve

Based on Table 3 and Figure 6, it can be seen that the spatial distribution of wheat threshed mixture on the cleaning sieve is not randomly formed, but closely related to the axial transport and radial throwing of material within the single longitudinal axial-flow threshing unit, as well as the physical characteristics of different components. Overall, the material distribution exhibits frontal concentration of plump grains, lateral offset of light impurities, and rear accumulation of stalk components.

Firstly, plump grains exhibit a clear front-concentrated distribution on the sieve. As shown in Table 3, the mass percentages of plump grains in the a-side and b-side regions at the front of the sieve differed markedly, with Zone 1-a containing 70.52% of the plump grains compared to 34.25% in Zone 1-b. This indicates that during the initial separation stage, plump grains are more likely to settle in the front-right region of the cleaning sieve. This phenomenon may be attributed to the combined effects of impact, rubbing, and combing by the drum teeth, as well as the relatively high density and inertia of plump grains. These characteristics allow plump grains to pass through the concave and deposit preferentially in the front-right region of the cleaning sieve corresponding to the descending side of the drum under the combined effects of tangential throwing and centrifugal action. Consequently, Zone 1-a becomes the primary deposition area for plump grains. As the material moves backward along the drum axis, the proportion of plump grains gradually decreases, forming a front-concentrated and rear-sparse longitudinal distribution pattern

Secondly, the distribution of chaff and light impurities shows certain differences compared to grains. In Zone 1-b, the mass percentage of chaff and light impurities reaches 47.24%, significantly higher than the 24.30% in Zone 1-a at the same axial location. This indicates lateral segregation occurs as materials fall through the concave sieve, with light impurities more likely to accumulate on the left side. Compared to plump grains, light impurities and broken leaves have lower bulk density and smaller particle mass, resulting in lower critical terminal velocities, making them more susceptible to displacement by internal airflow and vortex effects. Under the combined influence of tangential ejection and centrifugal forces, light components are prone to delayed settling or lateral drift, resulting in higher mass percentages on the b-side.

Thirdly, stalk components primarily exhibit longitudinal accumulation and delayed settling. As shown in Table 3, the mass percentages of long and short stalks in Zone 1-b are 4.72% and 3.94%, respectively, while in Zone 3-b, they increase to 16.27% and 17.06%, summing to 33.33%. This indicates that stalks, due to larger size, irregular shape, and higher flexibility, are slower to descend through the concave, following longer axial transport paths within the drum. The impact from drum rasp bars, brushing, and axial guidance further delays the settling, increasing the relative proportion of stalks in the rear regions of the sieve.

In summary, the axial transport and radial throwing jointly influence the deposition patterns of wheat threshed mixture on the cleaning sieve. Different components exhibit differentiated settling behavior due to variations in density, shape, size, and terminal velocities. These results are consistent with previous findings that guide vanes affect axial transport and separation within longitudinal axial-flow threshing drums [5]. Furthermore, analyzing the mass distribution across sieve regions quantitatively reveals the existence of high-load zones and heterogeneous component composition. This spatial heterogeneity implies that uniform airflow may fail to simultaneously satisfy the penetration requirements for high-load areas and the low-loss cleaning requirements for low-load areas. Therefore, integrating the critical terminal velocity characteristics of different components is essential for determining cleaning airflow velocity boundaries and developing zone-differentiated airflow control strategies.

3.2. Critical Terminal Velocity Characteristics of Components and Cleaning Airflow Velocity Boundaries

Based on the spatial distribution characteristics of the wheat threshed mixture on the cleaning sieve, the critical terminal velocities of the main components were measured to further analyze the matching relationship between cleaning airflow parameters and material components. The tested components included plump grains, unthreshed heads, long stalks, short stalks, and chaff and light impurities. According to the method described in Section 2.3.3, the critical terminal velocity of each component was measured using the critical terminal velocity test apparatus.

During the test, 50 samples were randomly selected from each component for repeated measurements. When each sample reached a relatively stable suspended state in the vertical upward airflow, the corresponding dynamic pressure was recorded, and the critical terminal velocity was calculated according to Eq. (8). The typical components of the wheat threshed mixture are shown in Figure 7. The critical terminal velocity test process is shown in Figure 8. The statistical results are listed in Table 4.

(a) (b) (c) (d) (e)

Figure 7. Typical components of the wheat threshed mixture. (**a**) plump grains; (**b**) unthreshed heads; (**c**) long stalks; (**d**) short stalks; and (**e**) chaff and light impurities.

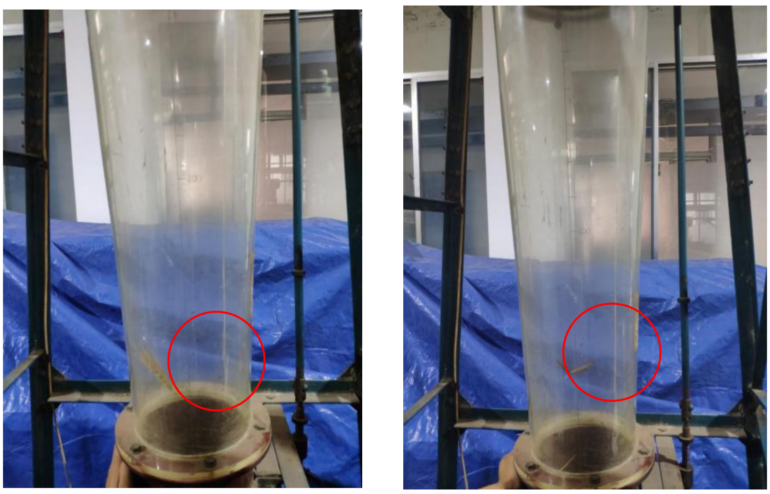

Figure 8. Critical terminal velocity test of wheat threshed components.

Table 4. Critical terminal velocities of wheat threshed components.

Component	Sample size(n)	Critical terminal velocity range / *m/s*	Average critical terminal velocity / *m/s*	CV /(%)
Plump grains	50	6.85 - 8.12	7.51 ± 0.32^{a}	4.32
Long stalks	50	4.50 -6.80	6.13 ± 0.44^{b}	7.21

Unthreshed heads	50	4.95 - 6.25	5.65±0.29[c]	5.18
Short stalks	50	3.55 -4.88	4.22±0.27[d]	6.45
Chaff and light impurities	50	1.65-2.45	2.12±0.19[e]	8.76

Note: Values followed by different lowercase letters (a–e) within the same column indicate significant differences at $p < 0.05$ (Duncan's multiple range test).

The results showed that plump grains had the highest critical terminal velocity, with an average value of 7.51 *m/s*. This was followed by long stalks, unthreshed heads, short stalks, and chaff and light impurities, with average values of 6.13, 5.65, 4.22, and 2.12 *m/s*, respectively. The ANOVA results showed significant differences in critical terminal velocity among the components ($P < 0.05$). The order of critical terminal velocities was as follows:

$$V_{\text{grain}} > V_{\text{long stalk}} > \mathrm{V}_{\text{unthreshed heads}} > V_{\text{short stalk}} > V_{chaff\ and\ light\ impurities} \tag{9}$$

These results indicate that different components of the wheat threshed mixture respond differently to cleaning airflow. Chaff and light impurities, which had the lowest critical terminal velocity, were the easiest components to be suspended and removed by airflow. In contrast, plump grains and long stalks had higher critical terminal velocities and were less likely to be carried out under the same airflow condition. Unthreshed heads had an intermediate critical terminal velocity, lower than those of plump grains and long stalks but higher than those of short stalks and chaff and light impurities. Since unthreshed heads are recoverable materials that should enter the rethreshing process rather than be discharged from the cleaning chamber, their critical terminal velocity is important for determining the upper boundary of cleaning airflow velocity.

Regarding the lower boundary of cleaning airflow velocity, chaff and light impurities had the lowest critical terminal velocity, with an average value of 2.12 *m/s*. When the airflow velocity is lower than this value, chaff and light impurities are difficult to suspend and remove effectively, which may increase the impurity content of harvested grains. Therefore, 2.12 *m/s* can be regarded as the theoretical lower boundary for effective removal of light impurities.

Regarding the upper boundary of cleaning airflow velocity, unthreshed heads had a critical terminal velocity of 5.65 *m/s*. Although plump grains and long stalks had higher critical terminal velocities of 7.51 and 6.13 *m/s*, respectively, they should not be used as the direct basis for determining the upper boundary of the cleaning airflow velocity. Plump grains are the target product and should be protected from airflow entrainment, whereas long stalks are primarily discharged through the combined mechanical actions of sieve vibration, material conveying, and tail-sieve discharge, rather than being removed primarily by airflow suspension. Therefore, the higher critical terminal velocity of long stalks does not represent the allowable upper limit of the cleaning airflow. In contrast, unthreshed heads are recoverable materials that still contain grains and should enter the rethreshing process. If the airflow velocity exceeds their critical terminal velocity, unthreshed heads may be carried out of the cleaning chamber, resulting in recoverable grain loss. Therefore, the critical terminal velocity of unthreshed heads, 5.65 *m/s*, was used as the theoretical upper boundary for low-loss cleaning airflow.

Based on the above analysis, considering both the removal of chaff and light impurities and the recovery of unthreshed heads, the theoretical control range of cleaning airflow velocity was preliminarily estimated to be 2.12-5.65 *m/s*. Within this range, the lower boundary corresponds to the airflow requirement for suspending and removing chaff and light impurities, whereas the upper boundary corresponds to the airflow limit for preventing recoverable unthreshed heads from being carried out of the cleaning chamber. This velocity range provides an aerodynamic basis for the subsequent analysis of the matching relationship between cleaning airflow and non-uniform sieve load.

3.3 Analysis of Zone-Differentiated Airflow Control Based on Sieve Load and Suspension Characteristics

Based on the spatial distribution characteristics of the wheat threshed mixture on the cleaning sieve and the critical terminal velocity characteristics of the main components, the coupling relationship between sieve load and component suspension behavior was further analyzed. Under the single longitudinal axial-flow condition, the wheat threshed mixture exhibited both spatial load non-uniformity and component-specific separation characteristics on the cleaning sieve. Therefore, the cleaning airflow should not be regulated only according to a single uniform airflow velocity, but should be adjusted by considering both regional sieve load and component suspension characteristics.

As shown in Table 3 and Figure 6, the front-right region of the sieve, namely Zone 1-a, was the primary deposition region for plump grains, with a mass percentage of 70.52%. This indicates that Zone 1-a may be prone to forming a locally high-load material layer. Under this condition, the material layer may increase airflow penetration resistance and reduce the effective airflow velocity acting on light impurities inside the layer. Therefore, high-load regions require sufficient airflow penetration to loosen the material layer and promote the separation and removal of chaff and light impurities.

However, the airflow velocity in high-load regions cannot be increased without limitation. According to the critical terminal velocity results in Section 3.2, the theoretical airflow velocity range for effective impurity removal and low-loss cleaning was preliminarily estimated to be 2.12-5.65 *m/s*. The lower boundary of 2.12 *m/s* corresponds to the minimum airflow requirement for suspending and removing chaff and light impurities, whereas the upper boundary of 5.65 *m/s* corresponds to the airflow limit for preventing recoverable unthreshed heads from being carried out of the cleaning chamber. Therefore, even in high-load regions, airflow regulation should enhance local penetration and distribution uniformity rather than simply increasing the overall airflow velocity beyond the theoretical upper boundary.

In contrast, low-load regions of the sieve have a thinner material layer and lower airflow penetration resistance. In these regions, excessive airflow may cause recoverable unthreshed heads to be carried out of the cleaning chamber, resulting in increased cleaning loss. Therefore, moderate airflow is sufficient for removing chaff and light impurities in low-load regions, while unnecessary airflow surplus should be avoided. This indicates that uniform airflow supply is difficult to simultaneously satisfy the airflow penetration requirement in high-load regions and the low-loss cleaning requirement in low-load regions.

Based on the above analysis, a zone-differentiated airflow control strategy is recommended for the cleaning system of a single longitudinal axial-flow wheat combine harvester. For high-load regions such as Zone 1-a, the airflow-guiding structure should enhance local airflow penetration and improve the fluidization of the material layer, thereby facilitating the separation of chaff and light impurities from plump grains. For low-load regions, airflow intensity should be appropriately reduced or maintained at a moderate level to avoid excessive entrainment of unthreshed heads while ensuring the removal of light impurities.

It should be noted that the mean-based theoretical airflow velocity range of 2.12-5.65 *m/s* was derived from the critical terminal velocities of individual components under vertical airflow conditions. This range provides an aerodynamic boundary for cleaning airflow parameter setting, but it should not be regarded as a fixed optimal operating velocity for all sieve regions. In actual cleaning operations, airflow velocity is also affected by material layer thickness, local sieve load, airflow direction, sieve vibration, and the structural layout of the cleaning chamber. Therefore, airflow regulation should integrate both the component critical terminal velocity characteristics and the spatial distribution of sieve load.

This analysis suggests that airflow distribution in the cleaning system of a single longitudinal axial-flow wheat combine harvester may be optimized according to regional sieve load and component separation characteristics. For high-load regions, increasing local airflow penetration may improve material-layer fluidization and facilitate the removal of chaff and light impurities. For low-load regions, moderate airflow may remove light impurities while reducing the risk of recoverable unthreshed heads being carried out of the machine. These results provide a theoretical reference for airflow-guiding structure design, air-duct optimization, and adaptive airflow-control strategies in non-uniform cleaning systems.

CONCLUSIONS

This study addressed the non-uniform distribution of threshed mixture on the cleaning sieve and the regional differences in material deposition during the cleaning process of a single longitudinal axial-flow wheat combine harvester. Using a self-developed 4LZ-2.5 longitudinal axial-flow threshing and cleaning test bench, experiments were conducted to investigate the spatial distribution of wheat threshed mixture on the cleaning sieve and the critical terminal velocities of key components. Based on the regional deposition characteristics and component critical terminal velocity characteristics, the theoretical control boundaries of cleaning airflow velocity were analyzed. The main conclusions are as follows.

(1) Under the single longitudinal axial-flow condition, the wheat threshed mixture exhibited a pronounced non-uniform spatial distribution on the cleaning sieve. Plump grains were mainly concentrated in the front-right region of the sieve, showing a transverse offset toward the descending side of the drum. In Zone 1-a, the mass percentage of plump grains reached 70.52%, which was markedly higher than that in the other zones, suggesting that this region may be prone to local material accumulation. In contrast, the mass percentage of chaff and light impurities in Zone 1-b reached 47.24%, higher than the 24.30% observed in Zone 1-a at the same longitudinal position. These results indicate that, during the single longitudinal axial-flow threshing and separation process, the threshed mixture was non-uniform in both deposition pattern and component composition across different sieve regions.

(2) The critical terminal velocities differed markedly among the different components of the wheat threshed mixture. The average critical terminal velocities of plump grains, long stalks, unthreshed heads, short stalks, and chaff and light impurities were 7.51, 6.13, 5.65, 4.22, and 2.12 *m/s*, respectively. Chaff and light impurities had the lowest critical terminal velocity, indicating that 2.12 *m/s* can be regarded as the theoretical lower boundary required for effective removal of light impurities. The critical terminal velocity of unthreshed heads was lower

than those of plump grains and long stalks, indicating that unthreshed heads are the sensitive component limiting the upper boundary of cleaning airflow velocity. Considering both the removal of chaff and light impurities and the recovery of unthreshed heads, the mean-based theoretical control range of cleaning airflow velocity was preliminarily estimated as 2.12-5.65 *m/s*.

(3) Coupling the spatial distribution of sieve load with the critical terminal velocity characteristics of different components showed that a single uniform airflow field cannot simultaneously satisfy the airflow penetration requirement in high-load regions and the low-loss cleaning requirement in low-load regions. For high-load regions such as Zone 1-a, local airflow penetration may need to be enhanced to improve material-layer fluidization and promote the separation of light impurities. For low-load regions, excessive airflow should be avoided to reduce the risk of recoverable unthreshed heads being carried out of the cleaning chamber. These results indicate that a zone-differentiated airflow distribution strategy based on sieve load and component suspension characteristics can provide a reference for parameter setting and structural optimization of non-uniform airflow cleaning systems in single longitudinal axial-flow wheat combine harvesters.

It should be emphasized that the mean-based theoretical range of 2.12-5.65 m/s estimated in this study represents a theoretical control boundary derived from the measured critical terminal velocities of individual components under vertical airflow conditions. It is not equivalent to the optimal operating airflow velocity under actual harvesting conditions. This range should be further validated against cleaning loss, impurity content, and unthreshed-head recovery rate under different zone-differentiated airflow combinations. Future studies should conduct zonal airflow regulation tests and incorporate cleaning performance indicators to optimize and experimentally validate the zone-differentiated airflow distribution strategy under non-uniform load conditions.

Funding: This research was funded by the National Key Research and Development Program of China, grant number 2021YFD2000503, and the Jiangsu Province Frontier Leading Technology Program, grant number BF2025311.
Conflicts of Interest: The authors declare no conflict of interest.

REFERENCES

[1] SHIFERAW B, SMALE M, BRAUN H-J, et al. Crops that feed the world 10. Past successes and future challenges to the role played by wheat in global food security [J]. Food security, 2013, 5(3): 291-317.

[2] LIANG Z, WADA M E. Development of cleaning systems for combine harvesters: A review [J]. Biosystems Engineering, 2023, 236: 79-102.

[3] DUMBRAVĂ I-A, CâRLESCU P-M, ROȘCA R, et al. Installation and Advanced Method for the Evaluation of Air Velocity over the Sieves of the Cleaning Unit of Combine Harvesters [J]. Agriculture, 2025, 15(20): 2173.

[4] YUAN L, HE X, ZHU C, et al. Design and test of tangential and longitudinal-axial threshing and separating unit for wheat [J]. Results in Engineering, 2024, 21: 101774.

[5] MILIŠAUSKAS M, PETERSEN N, MILIŠAUSKIENĖ G, et al. Crop Flow Control in a Longitudinal Axial Threshing Unit Using Fully Adjustable Guide Vanes: A Field Study in Winter Wheat Harvesting [J]. Applied Sciences, 2025, 15(12): 6864.

[6] GORIAL B, O'CALLAGHAN J. Aerodynamic properties of grain/straw materials [J]. Journal of Agricultural Engineering Research, 1990, 46: 275-90.

[7] KHOSHTAGHAZA M, MEHDIZADEH R. Aerodynamic properties of wheat kernel and straw materials [J]. 2006.

[8] ZEWDU A. Aerodynamic properties of tef grain and straw material [J]. Biosystems engineering, 2007, 98(3): 304-9.

[9] BADRETDINOV I D, MUDARISOV S G, KHALIULLIN D T. Examination of the Airflow Uneven Distribution over the Combine Harvester Cleaning System [J]. Mathematical modelling of engineering problems, 2022, 9(2):371-378.

[10] ZHOU X, WANG Z, TIAN L, et al. Numerical Simulation and Experiment of Cleaning Performance of Combine Harvester under the Action of Conical Fan [J]. Engineering in Agriculture, Environment and Food, 2022, 15(2): 61-71.

[11] STREICHER E, STROSHINE R, KRUTZ G, et al. Cleaning shoe air velocities in combine harvesting of wheat [J]. Transactions of the ASAE, 1986, 29(4): 923-928.

[12] CRAESSAERTS G, SAEYS W, MISSOTTEN B, et al. Identification of the cleaning process on combine harvesters. Part I: A fuzzy model for prediction of the material other than grain (MOG) content in the grain bin [J]. Biosystems Engineering, 2008, 101(1): 42-9.

[13] BADRETDINOV I, MUDARISOV S, LUKMANOV R, et al. Mathematical modeling and research of the work of the grain combine harvester cleaning system [J]. Computers and Electronics in Agriculture, 2019, 165: 104966.

[14] CHAI X, XU L, SUN Y, et al. Development of a cleaning fan for a rice combine harvester using computational fluid dynamics and response surface methodology to optimise outlet airflow distribution [J]. Biosystems Engineering, 2020, 192: 232-44.

[15] LIANG Z, XU L, DE BAERDEMAEKER J, et al. Optimisation of a multi-duct cleaning device for rice combine harvesters utilising CFD and experiments [J]. Biosystems Engineering, 2020, 190: 25-40.

[16] LIANG Y, TANG Z, ZHANG H, et al. Cross-flow fan on multi-dimensional airflow field of air screen cleaning system for rice grain [J]. International Journal of Agricultural and Biological Engineering, 2022, 15(4): 223-35.

[17] YIN J, CUI Y, ZHA Z, et al. Study and Testing of a Front-Blowing and Rear-Suction Enhanced Cleaning Technology for Grain Combine Harvesters [J]. Agriculture, 2025, 15(16): 1722.

[18] LI D, HE Q, YUE D, et al. Research and experiment on airflow field control technology of harvester cleaning system based on load distribution [J]. Agriculture, 2024, 14(5): 779.

[19] LIU P, JIN C, NING X, et al. Field performance test and analysis of the cleaning sieve of soybean harvesters [J]. Transactions of the CSAE, 2020, 36(9): 36-43.

[20] LIU P, WANG X, JIN C. Bench test and analysis of cleaning parameter optimization of 4 L-2.5 wheat combine harvester [J]. Applied Sciences, 2022, 12(18): 8932.

[21] LIU P, WANG X, JIN C. Research on the adaptive cleaning system of a soybean combine harvester [J]. Agriculture, 2023, 13(11): 2085.

[22] PEI E-P, CHENG F, WANG X, et al. Design and test of cleaning device of oat thresher [J]. 2022, 50(5):737–747

[23] SHI R, DAI F, ZHAO W, et al. Optimal design and testing of a crawler-type flax combine harvester [J]. Agriculture, 2023, 13(2): 229.

[24] ZIHENG Z, GUIXIANG T, SHUJUAN Y, et al. Design and experimental of a wind sieve type cleaning device for cereals [J]. Journal of Chinese Agricultural Mechanization, 2024, 45(6): 119.

[25] AJMAL U, KHAN M, FAHEEM M, et al. Modification and performance evaluation of a wheat thresher [J]. Russian Journal of Agricultural and Socio-Economic Sciences, 2017, 65(5): 261-70.

[26] DING B, LIANG Z, QI Y, et al. Improving cleaning performance of rice combine harvesters by DEM–CFD coupling technology [J]. Agriculture, 2022, 12(9): 1457.

[27] DU X, NI K, CHEN J, et al. Numerical simulation and experiment of gas-solid two-phase flow in a cross-flow grain cleaning device; proceedings of the 2013 Kansas City, Missouri, July 21-July 24, 2013, F, 2013 [C]. American Society of Agricultural and Biological Engineers.

[28] LI Y, XU L, LV L, et al. Study on modeling method of a multi-parameter control system for threshing and cleaning devices in the grain combine harvester [J]. Agriculture, 2022, 12(9): 1483.

[29] YUE D, WANG Q, HE Q, et al. A study of the distribution of the threshed mixture by a double longitudinal axial flow corn threshing device [J]. Agriculture, 2024, 14(2): 166.